Development of Flow Structures in the Lee of an Inclined Body of Revolution

K. C. Ward* and J. Katz†
Purdue University, West Lafayette, Indiana

Laser-induced fluorescence has been utilized for visualizing the flow structures behind an inclined body of revolution in a large towing tank. The observations have focused on the effects of the incidence angle and the Reynolds number on the axial development of the large-scale structures within the separated region, as well as the location of boundary-layer separation and reattachment. At low angles of incidence and low Reynolds numbers, the flow is symmetric, containing two large centers (foci) of coalescencing stream surfaces as well as several secondary structures. The transition to an asymmetric flow is observed to begin first in the downstream sections with the gradual detachment of the left primary center and an inward motion of the right-hand center. While detaching, the primary left structure becomes elongated as the stream surfaces break and coalesce into two distinct centers. The resulting two foci start interlacing further downstream and eventually recombine. When the left center of coalescence is completely detached, an additional center forms in its place and the right-hand structure starts lifting away from the surface. Evidence of asymmetry very close to the tip of the model at 45 deg incidence is also provided. Finally, this paper includes a series of qualitative drawings of the flow topology, which follow the evolution of the flow structures in the lee of the model.

Introduction

THE existence of either symmetric or asymmetric wake structures in the lee of an inclined body of revolution, depending on the incidence angle, Reynolds number, model geometry, tip bluntness, freestream turbulence, and even the roll angle, has been well established.[1-10] The transition from a symmetric to an asymmetric wake usually occurs when the incidence angle is about twice the half-apex angle of the nose cone[6] and the Reynolds number is above a threshold value. For a 3.5 l/D ogive (l being the length of the nose cone and D the base diameter), which is the test body of the present work, this rule implies that transition to asymmetric flow occurs at about 30 deg incidence. The occurrence of asymmetry induces an uneven pressure distribution on the surface of a model that results in the generation of an adverse side force. Locally, this side force can reach a value of 2.2 times the normal force and globally it can reach a value of about 1.5 times the overall normal force.[11] The pioneering research on the development of these side forces, and the flow structures that induce them, has been performed by Allen and Perkins.[1,2] Their studies have provided general information about the behavior of the large-scale structures within the wake and led to a hypothesis known as the "crossflow analogy." This analogy compares the axial development of the wake structures behind an inclined body of revolution to the development, with time, of the vortex structures behind an impulsively started two-dimensional cylinder. Since then, this problem has been studied extensively[12-22] and several reviews have also been written.[11,23-26] Attempts to solve this problem numerically have focused on Euler and Reynolds-averaged Navier-Stokes methods[16] as well as ad hoc forms of the crossflow analogy.[17]

Most of the past experimental research[3-10] has focused on determining the affects of the controlling parameters on the force and pressure distributions. Several flow visualization techniques, such as schlieren photography,[3,4] vapor screens,[2,19] and wool tuft grids[5,9] have also been applied while trying to observe the details of the wake structures of various bodies of revolution. Quantitative measurements, such as laser Doppler velocimeter (LDV) surveys,[12,14] have also been performed. The available information, however, is limited since the LDV system measures the velocity at a particular point. As a result, an intricate survey of such a complicated flowfield, at various Reynolds numbers and incidence angles, is cumbersome and virtually impossible. These difficulties have triggered some simultaneous investigations combining flow visualization, force measurements, and velocity surveys.[18-22] However, these combined measurements have been performed at a limited number of incidence angles and Reynolds numbers (two different freestream velocities by Yanta and Wardlaw[21] and two by Schwind and Mullen[18]). The studied cross sections have also been located at the cylindrical afterbody and limited to regions away from the model's surface. As the present paper will show, many details of the wake structure, particularly around the nose cone, have not yet been identified.

One of the primary reasons for the lack of detailed information on the flow structure in the lee of the model is the difficulty in visualizing the flow. Of the various techniques of flow visualization, we have already mentioned schlieren photography, the wool tuft, and the vapor screen. These methods provide only a rough and qualitative image of the flowfield and cannot identify the fine details of the flow geometry. Surface flow visualization[15,25] is limited to the flow pattern in a close vicinity to the model's surface and cannot, by itself, identify the flow structures that cause a particular pattern. Thus, very little is known about their initial stages of development, the effect of Reynolds number and incidence angle on the exact flow geometry, the physical appearance of the primary and secondary structures, etc. To achieve these objectives, one must be capable of visualizing the flow in detail at various sections and observe the effects of the above-mentioned parameters. Flow visualization has received increased attention in recent studies of complex vortex flows.[27,28] Of the existing techniques, the most promising is laser-induced fluorescence,[29,30] namely, illu-

Presented as Paper 87-2276 at the AIAA 5th Applied Aerodynamics Conference, Monterey, CA, Aug. 17-19, 1987; received Aug. 26, 1987; revision received May 30, 1988.

*Graduate Student, Hydromechanics Laboratory, School of Civil Engineering; currently at Johns Hopkins University, Baltimore, MD.

†Assistant Professor, Hydromechanics Laboratory, School of Civil Engineering; currently at Johns Hopkins University, Baltimore, MD.

minating the wake of a model with a laser sheet and distributing fluorescing dye in the freestream. As a result, this technique has been adopted to the present study.

This paper summarizes a series of observations on the flow structures in the lee of an inclined body of revolution. The experiments have focused on the wake development in the lee of a rigidly mounted 10 in. base diameter D, 3.5 l/D tangent ogive, with a sharp tip. The flow has been studied at incidence angles of 25–55 deg and Reynolds numbers (based on the base diameter) between 7.8×10^3 and 4.0×10^5.

Description of the Experimental Setup

The flow visualization experiments have been performed in a 156 ft long towing tank with an 11×5 ft cross section. This facility is equipped with a carriage capable of moving at speeds up to 12.5 ft/s. As is evident from the sketch in Fig. 1, a thin (approximately 0.5 mm) sheet of light is created by expanding an argon ion laser beam through a cylindrical lens, which is located at the base of the illuminating optics strut. This laser sheet illuminates a verticle slice of the flowfield, which is perpendicular to the direction of travel. When the water in the tank is carefully seeded with a fluorescing dye (Rhodamine 6G), the details of the flow structures within the laser sheet become visible, unobstructed by dye in the rest of the flowfield. A high-resolution video camera is focused on the laser sheet through a system of lenses contained in a submerged periscope (located in the camera strut), which trails approximately 10 ft behind the laser sheet. The images collected by the video camera are recorded on a high-resolution VCR. The magnification of the image can be controlled through the proper choice of lenses, so that the area shown on the video monitor ranges from 1×1 to 20×20 in. Further details of the experimental setup are provided in Refs. 31 and 32.

A substantial effort has been invested in insuring that the present results are repeatable and represent flow phenomena that characterize the model and not the geometry of the test facility or the experimental procedures. The layover time between runs has been established to be at least 1 h in order to insure that any secondary flow within the tank is reduced to an insignificant level. The low-speed experiments, however, have required a longer recess, sometimes a whole day. The effect of secondary tank flows on the experimental results is demonstrated by way of the two photographs shown in Figs. 2 and 3. At a very low carriage speed, such as 0.1 ft/s, and at 45 deg incidence, the flow structure remains symmetric within the upstream sections of the model, as shown in Fig. 2. However, beyond $x/D = 1.5$ (x being the axial distance from the tip), the flow becomes more and more sensitive to external disturbances and, as a result, the existence of secondary flows can cause a transition to the structure shown in Fig. 3. If the same run is performed after letting the water settle for several hours, the image at $x/D=2.0$ resembles the image shown in Fig. 2. An increase in the carriage speed, at approximately the same level of freestream disturbances (determined by the layover time between runs), vertical 0.2 ft/s is also sufficient to bring the lee flow structure back to a symmetric pattern. A few additional comments referring to the effect of repeating the experiments at a higher frequency are discussed later.

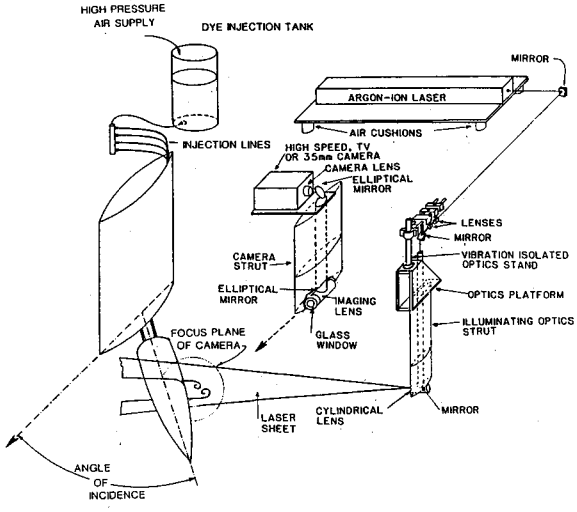

Fig. 1 Functional sketch of the flow visualization system.

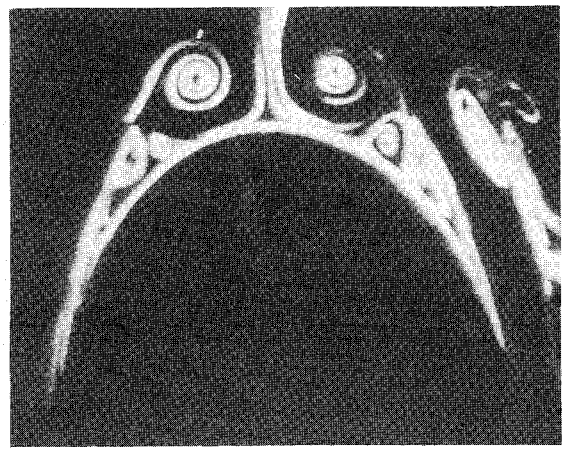

Fig. 2 Photograph of symmetric primary and secondary centers of coalescing stream surfaces in the lee of a 3.5 l/D ogive, with a sharp tip ($\alpha=45$ deg, $x/D=1.0$, and $Re_D=7.9\times10^3$).

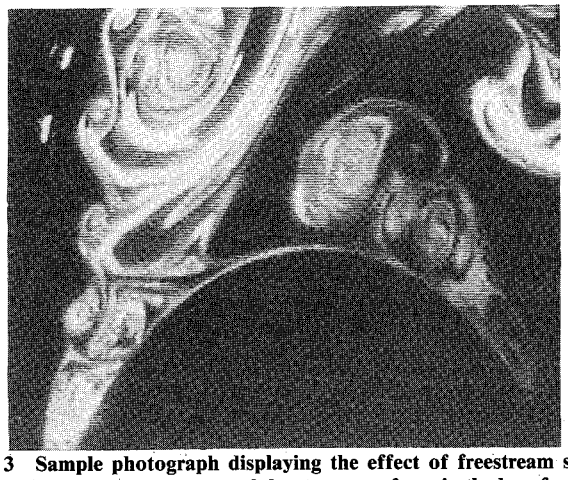

Fig. 3 Sample photograph displaying the effect of freestream secondary flows on the geometry of the stream surfaces in the lee of a 3.5 l/D ogive, with a sharp tip ($\alpha=45$ deg, $x/D=2.0$, and $Re_D=7.9\times10^3$).

Several methods of distributing the dye have also been tried. They include varying the injection rates from the model's surface, utilization of a series of small injectors mounted on a separate slow-moving carriage, and distribution with handheld injectors. These trials have verified that, as long as the dye is seeded in small quantities and very slowly, its method of distribution has no bearing on the results. The actual experiments have been performed by seeding the water upstream of the model prior to each run. The experiments have also been repeated in various sections of the tank ranging 20–100 ft downstream of the point at which the carriage has reached a constant speed. This procedure has insured that the recorded images represent "steady" conditions. The actual measurements have been performed after the carriage has moved at least 60 ft at a constant speed. In spite of these precautions, each flow condition has also been tested several times to insure repeatability. As a result, an enormous amount of data has been collected and stored on video tapes. These data have been

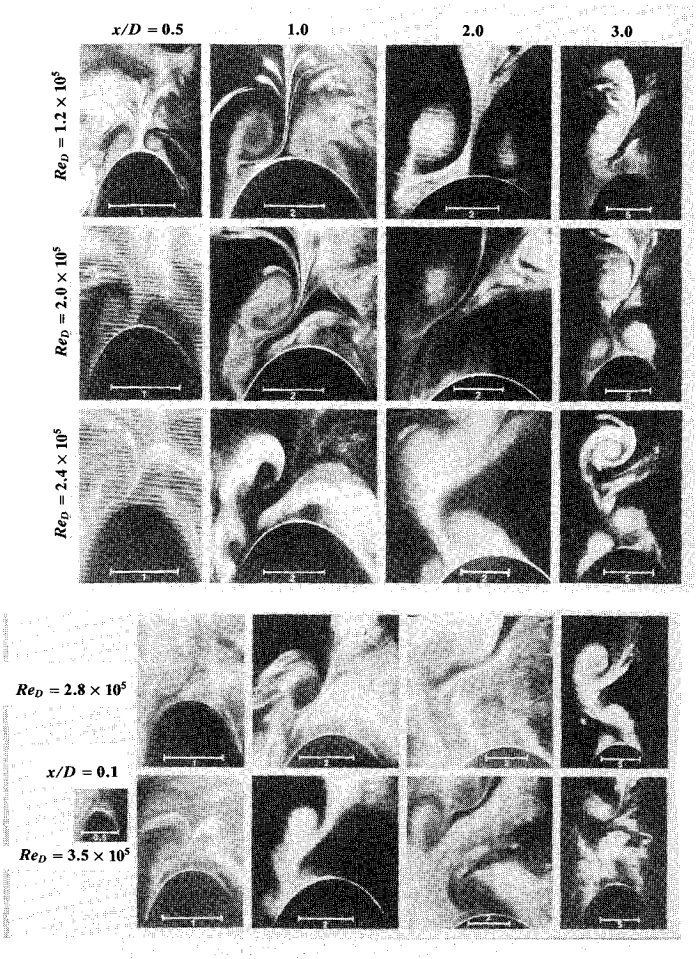

Fig. 4 Photographs showing the effects of the Reynolds number and the axial location on the wake structures for $\alpha = 45$ deg (the dimensions shown in the photographs are in inches).

studied carefully and numerous trends have been observed and documented. Obviously, the present paper can contain only a few sample photographs, as presented in Figs. 2–4, 7, and 9.

The observations, measurements, and analysis have been performed while examining the video records. Unlike still photographs, it has been possible to identify the motion of the fluid within the illuminated section by comparing successive video frames. Since the laser sheet crossects three-dimensional flow structures, the sample photographs actually show the intersection between the illuminated plane and stream surfaces within the separated region. For example, the video records that include the image shown in Fig. 2 make it possible to observe the motion of the fluid along the lines shown in this photograph. Thus, the velocity components within the illuminated plane are tangent to these lines. Each of the traces associated with the primary structure appears as a spiral and since it resembles a vortex (although the pattern is closer to a combination of a vortex and a sink), it has been widely referred to as a vortex by previous researchers.[1-32] However, in three dimensions, the fluid entrained by these structures actually moves along a path that resembles a converging helix. Thus, the stream surfaces associated with the large "vortex" coalesce into a single line whose intersection with the illuminated plane appears as the center (or focus) of the spiral. This argument may require us to redefine the names for the flow structures shown in Fig. 2 as "centers or foci of coalescence." The other alternative is to continue to call them "vortices," but then one should recognize that these structures do not have concentric cylindrical stream surfaces. We have opted to adopt the former term and from now on will refer to the "core" of these structures as the centers or foci of coalescencing stream surfaces.

Presentation of Results

A summary of the observed trends of the flow structures (measured off the video monitor) with the Reynolds number, incidence angle, and axial location are presented in this section. Also summarized are the locations of boundary-layer separation, reattachment, secondary separation, and their trends with the various flow parameter. Finally, an attempt is made to sketch several typical images of the flow topology.

Several sample photographs demonstrating the development of the flow structure in the lee of the model at 45 deg incidence are presented in Fig. 4. Each column represents the trends with the Reynolds number at a fixed axial location, whereas each row demonstrates the development along the axis of the model. This paper does not contain similar sequences at other incidence angles, but the trends at 25, 35, and 40 deg are presented graphically (along with those of 45 deg) in Figs. 5 and 6. Figure 5 is an overall summary of the location of the primary centers of coalescence and Fig. 6 contains a few sample sketches demonstrating the evolution of the flow in the lee of the model. As is evident from these figures, both the incidence and the Reynolds number affect this flow.

At 25 deg incidence (first column of Fig. 5 as well as Figs. 6a and 6e), the two centers or foci of the coalescencing stream surfaces remain quite symmetric (similar to Fig. 2) throughout the present range of Reynolds numbers. The only visible trend is a migration of the centers toward the leeward meridian at $x/D = 3.0$. As the incidence angle is increased to 35 deg the symmetric flow geometry persists up to $Re_D = 1.2 \times 10^5$. At higher velocities, the left-hand focus starts lifting away from the surface, while the right one moves toward the leeward meridian. The traces of asymmetry become visible first at $x/D = 3.0$ and, as the velocity is increased, they propagate upstream. These trends are clearly visible in the second column of Fig. 5, and by comparing Figs. 5 and 6b–6f. Note also that the primary changes in the wake structure occurs between $Re_D = 1.2 \times 10^5$ and 2.0×10^5. Within this range, an additional center of coalescence becomes clearly visible at $x/D = 3.0$ on the left-hand side of the leeward meridian, within the space vacated by the detaching initial structure. It should be noted here that the specific range of Reynolds numbers, at which the transition from a dual to a triple pattern occurs, seems to depend strongly on the existence of freestream secondary flows. When the same experiments have been repeated at a high frequency, without allowing the water in the tank to settle, this transition has been delayed and has started only at $Re_D = 2.4 \times 10^5$. The same peculiar sensitivity has been noticed also at higher incidence angles. It confirms previous suspicions[10] about the effect of the freestream turbulence on the development of the wake.

As the incidence angle is increased to 40 deg and then to 45 deg, the traces of asymmetry appear at decreasing Reynolds numbers. The initial signs (first row of Fig. 4) appear again as a gradual lifting of the left primary center of coalescence and the motion of the right-hand center toward the leeward meridian. This process starts at $x/D = 3.0$ and propagates upstream as the velocity is increased. As the original center detaches from the surface, an additional large structure appears in its place (compare the upper two photographs of the last column of Fig. 4).

As the left primary structure detaches, it undergoes major changes in its shape, as is evident by examining, for example, the third row of Fig. 4 ($Re_D = 2.4 \times 10^5$). At $x/D = 0.5$, the flow is already asymmetric, but only a single primary structure is clearly visible on each side of the leeward meridian. At $x/D = 1.0$, the left-hand side contains three distinct centers, the bottom one is attached to the surface, while the other two are detached. Further downstream, only one detached center of coalescence is visible. At $x/D = 2.0$, this detached structure is elongated, while at $x/D = 3.0$ it has a distinct spiral shape. Similar trends, but at different stages of development, are demonstrated in the fourth and fifth rows of Fig. 4. At $Re_D = 2.8 \times 10^5$, the stream surface converging into the left

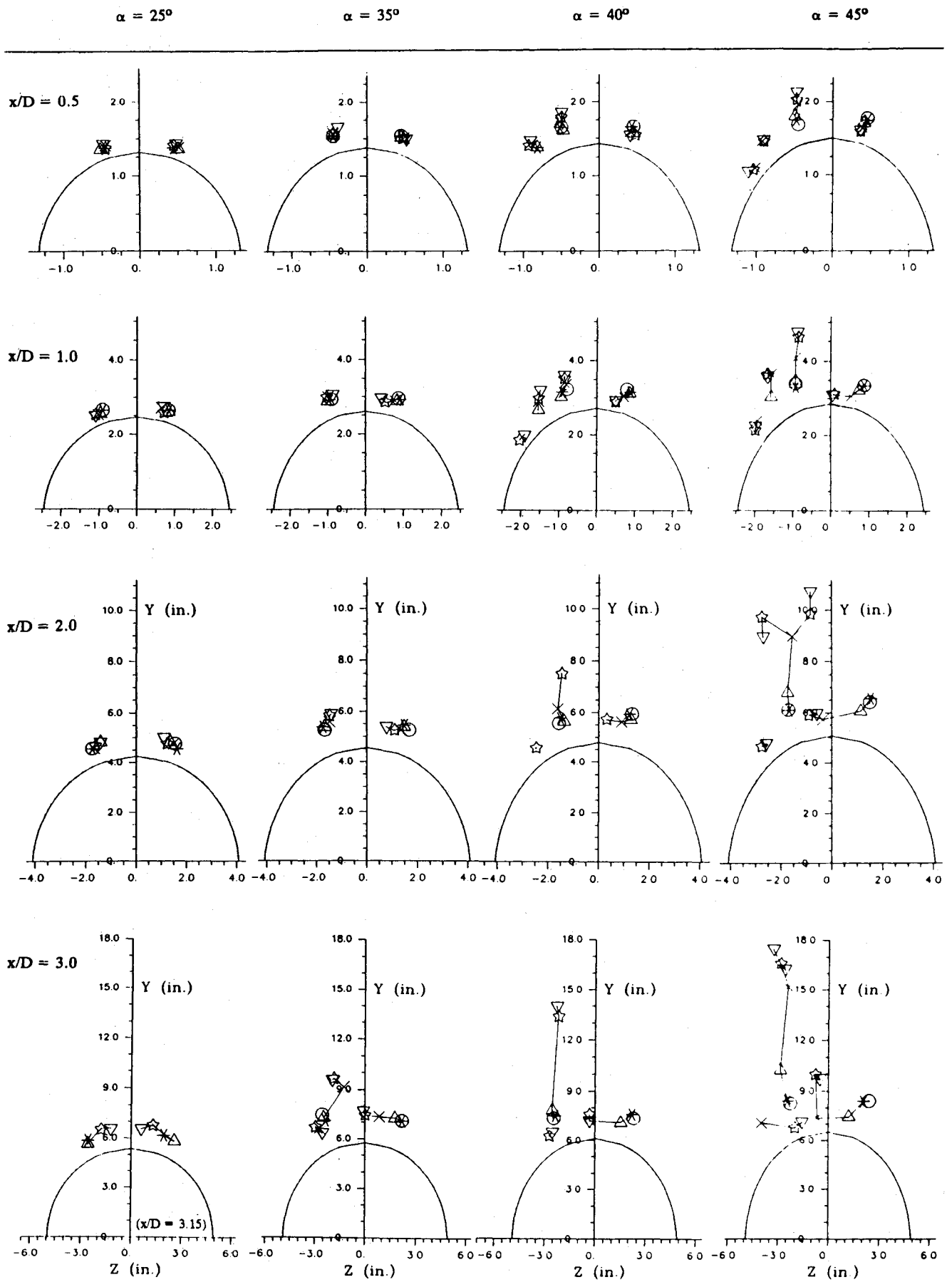

Fig. 5 Series of sketches illustrating the effects of the axial location and the incidence angle on the primary centers of coalescence: ○ $Re_D = 3.9 \times 10^4$, ✱ $Re_D = 7.9 \times 10^4$, △ $Re_D = 1.2 \times 10^5$, × $Re_D = 2.0 \times 10^5$, ○ $Re_D = 2.8 \times 10^5$, and ▽ $Re_D = 3.5 \times 10^5$.

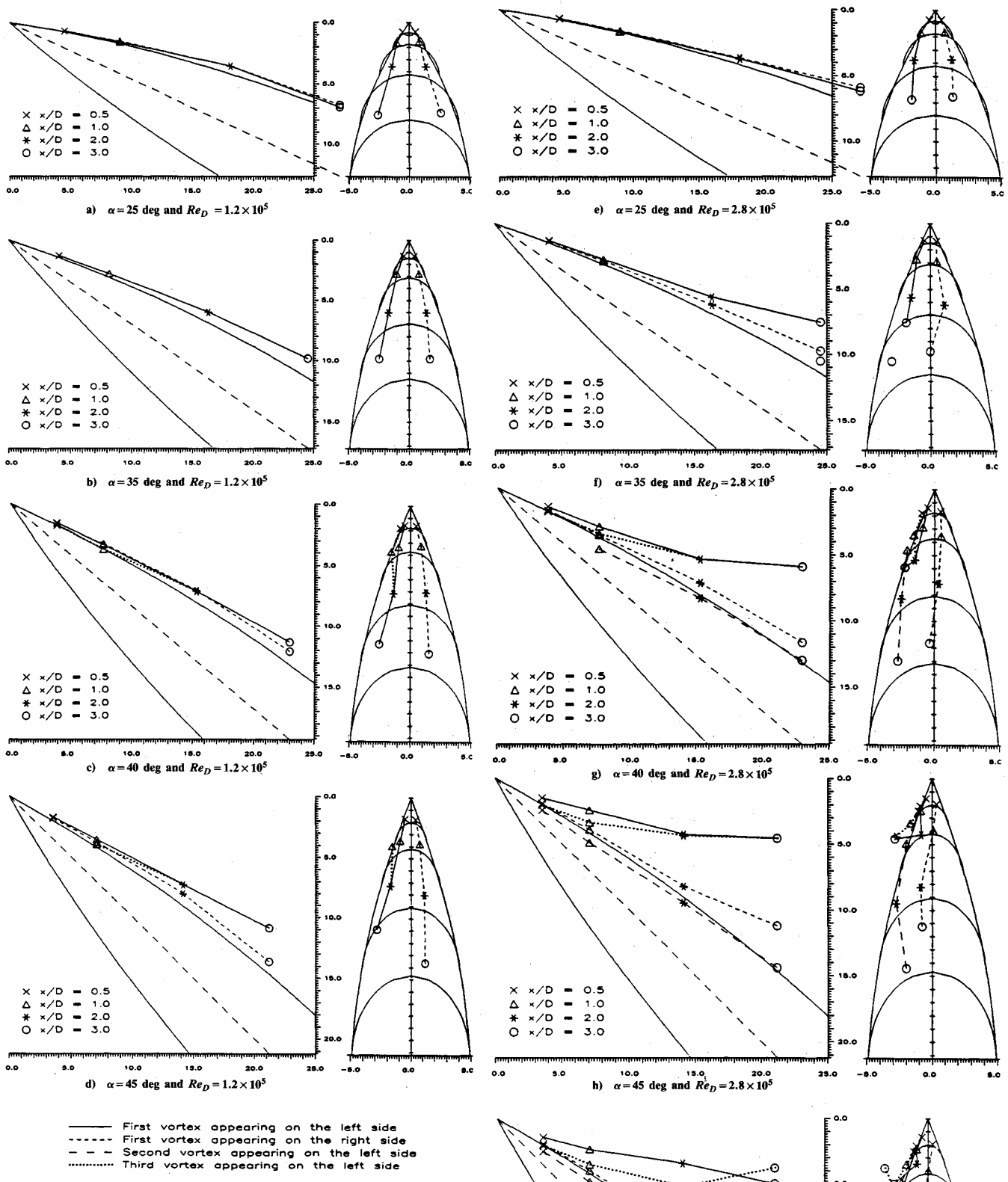

Fig. 6 Series of sketches illustrating the effects of the incidence angle and the axial location on the primary centers of coalescence (all scales are in inches).

primary center of coalescence already has an elongated shape at $x/D=0.5$ and three distinct structures appear on the left-hand side at $x/D=1.0$ and 2.0. Further downstream, at $x/D=3.0$, the two detached centers appear again as a single structure. In the last row of Fig. 4, the flow is already asymmetric at $x/D=0.1$ and two detached structures are already visible at $x/D=0.5$. These two centers of coalescence can be distinctly identified even at $x/D=3.0$ as they seem to rotate

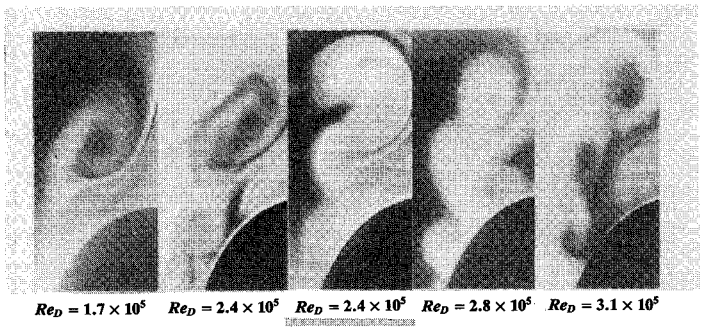

Fig. 7 Sequence of photographs demonstrating the changes in the flow structure at the same cross section, $x/D = 1$, ($\alpha = 45$ deg). This sequence demonstrates how the stream surfaces of the left primary structure.

around each other. Thus, the same process occurs in all the sequences of photographs, but as the Reynolds number is increased, the process starts further upstream and extends further downstream.

The transformation from a single, slightly detached structure, to a distinct pair of structures is also the focus of Fig. 7. This sequence demonstrates that as the Reynolds number is increased, the left primary structure becomes elongated and then splits when the stream surfaces "break" and start coalescing into two distinct centers. As the distance between these two structures and the body of the model increases (i.e., they begin to detach from the surface), a new structure forms close to the surface. As is evident from the last two columns of Fig. 4, the detached centers interlace around each other further downstream and eventually recombine into a single structure. Note that the process consisting of what seems to be a break in the stream surfaces, coalescence into two centers, and recombination at higher x/D is illustrated in Figs. 5, 6c, 6d, and 6g–6i. The same phenomena have been observed at 50 deg incidence, but they are not presented here due to the length of the paper. We will return to these phenomena while making an attempt to sketch the topology of this flow.

The process of vortex stretching and splitting has been reported very rarely in the literature. A theoretical prediction of splitting, when a vortex is exposed to high shear stresses, has been made by Moore and Saffman.[33] To the best of our knowledge, the only experimental evidence of vortex splitting has been observed by Freymuth et al.[34] behind a two-dimensional airfoil while being accelerated from rest. "Vortex" (or center of coalescence) stretching (but not splitting) behind an inclined body of revolution has also been detected by Oberkampf and Bartel[13] at low incidence angles (below 25 deg) and high Reynolds numbers (1.75×10^6).

The location of the lines of primary as well as secondary boundary-layer separation and reattachment are summarized in Fig. 8. At low velocities, as is evident from the photograph in Fig. 2, these points can be clearly identified. However, as the Reynolds number is increased, and the left primary center of coalescence starts lifting away from the surface, a peculiar phenomenon occurs. The line separating between the primary centers, which is so distinct in Fig. 2, seems to expand into a region containing a series of parallel lines that widen below the detaching primary structure (see Fig. 9). This region shrinks back to a narrow line when the center is completely detached and an additional structure develops in its place. For example, if one focuses on the third row of Fig. 4, the expansion to a wide region is evident at $x/D = 2.0$, and only a narrow line appears between the large structures at $x/D = 3.0$. The location of the expanded region between the primary structures is specified by the shaded areas in Fig. 8. A proposed explanation for this phenomenon is discussed while presenting the topology of this flow. These observations are also in agreement with a peculiar phenomenon that was observed by Keener[15] while performing oil flow studies on a similar model. His surface flow patterns contain a region with a varying thickness consisting of a series of oblique lines. Keener speculates, and the present observations confirm, that this region shrinks to the narrow line when a center of coalescence and the stream surfaces converging into it detach from the body and an additional structure forms in their place.

Several other trends can also be identified from Fig. 8. When the flow is symmetric (low Reynolds numbers and incidence angles), the primary separation point is located close to the lateral angle of 90 deg (0 and 180 deg are the windward and leeward meridians, respectively). As the left center starts lifting away from the surface and the right structure moves toward the leeward meridian, the reattachment point also migrates to the left and separation is delayed on the right side. When a new center develops in the space vacated by the original structure, the reattachment line starts migrating to the

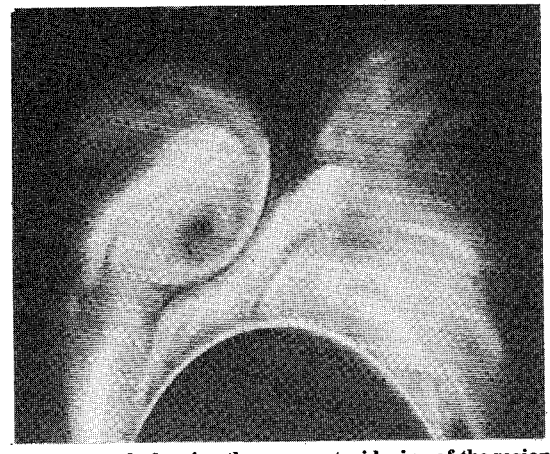

Fig. 8 Photograph showing the apparent widening of the region separating between the primary centers of coalescence, particularly ($\alpha = 45$ deg, $x/D = 1.0$, and $Re_D = 2.0 \times 10^5$.

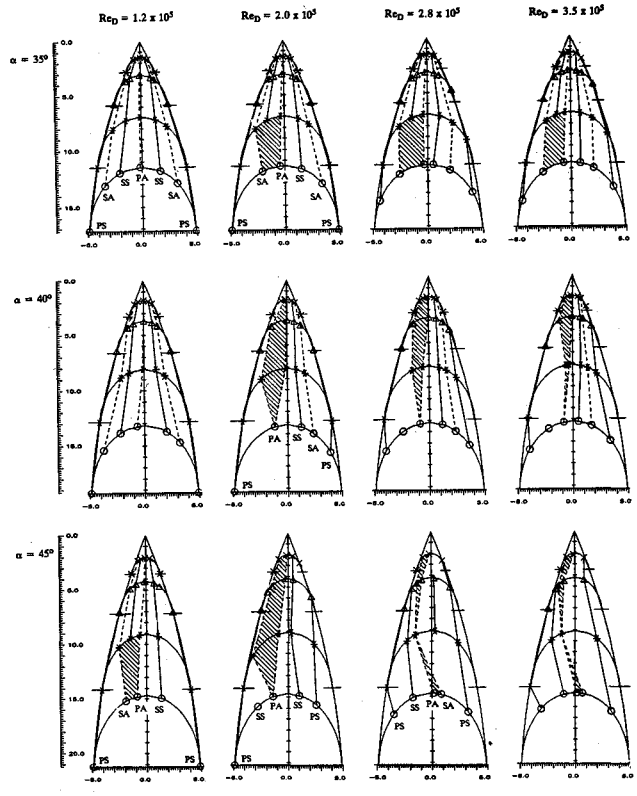

Fig. 9 The effects of the incidence angle and the Reynolds number on the lines of separation and reattachment: × $x/D = 0.5$, △ $x/D = 1.0$, * $x/D = 2.0$, ○ $x/D = 3.0$; (PS–location of primary separation, PA–primary attachment, SS–the secondary separation, SA– secondary attachment; — lines of separation; ——— lines of reattachment, shaded areas–apparent widening of the region separating between the primary centers of coalescence).

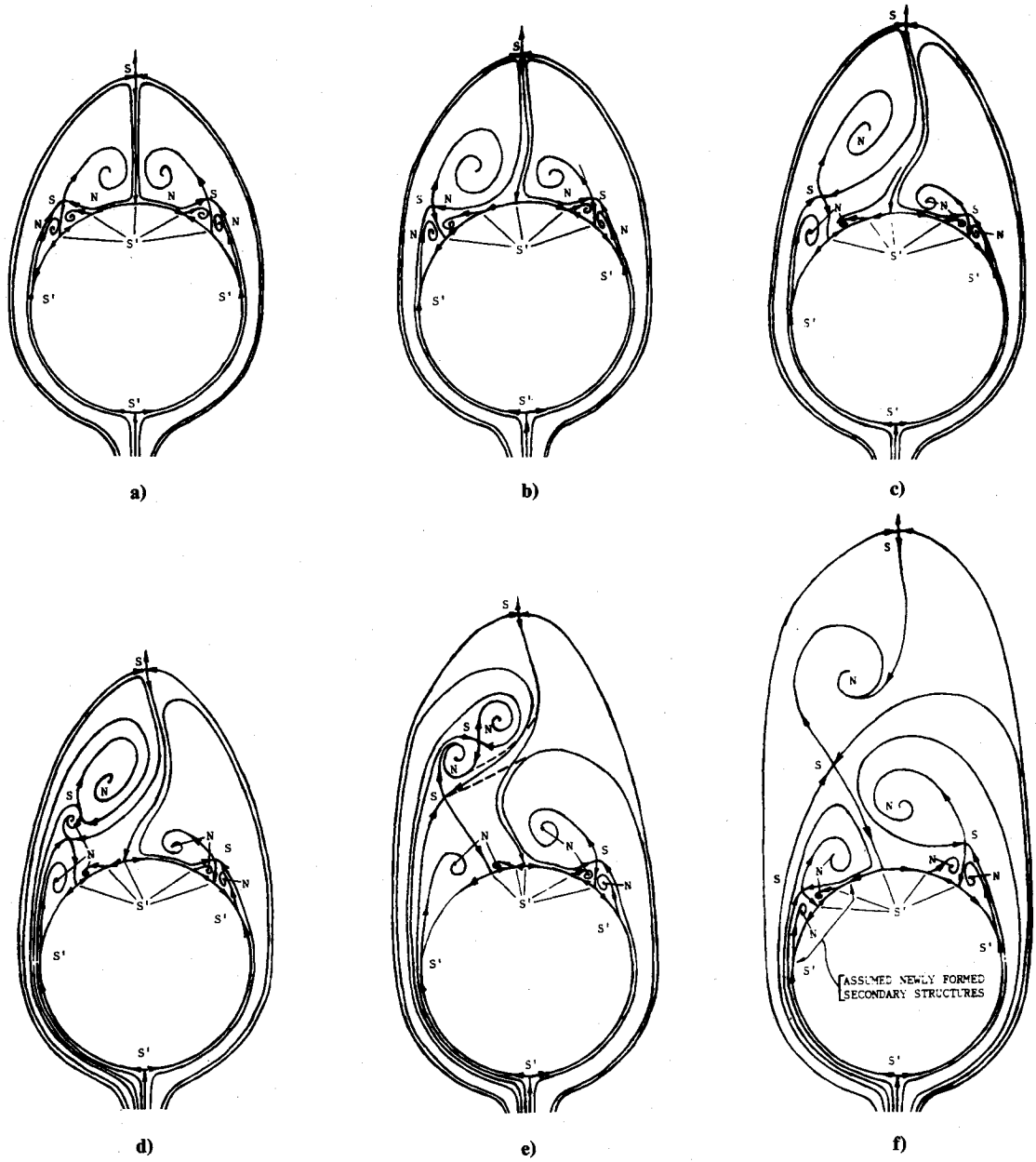

Fig. 10 Sketches of the topology of the wake structure in the lee of the inclined ogive: a) symmetric flow; b) early traces of asymmetry; c) further elongation of the left and motion of right primary structure toward the leeward meridian; d) the break in the stream surfaces of the left primary structure and coalescence into two centers; e) complete detachment of the split structures as well as the first traces of detachment of the right primary structures; and f) recombination of the split structures away from the surface, elongation of the detaching right primary center, and motion of the left center toward the leeward meridian.

right. Finally, as the right primary center detaches, this line crosses the leeward meridian, and separation is also delayed on the left-hand side.

Based on the current observations, an attempt has been made to sketch the topology of the flow structure in the lee of the model following the guidelines of Tobak and Peake.[35] A series of these sketches, which demonstrate the evolution of the centers of coalescence or foci is presented in Fig. 10. This series starts with a symmetric pattern (Fig. 10a), which contains multiple primary and secondary centers (nodes) as well as the appropriate number of saddle points. This sketch corresponds to the image shown in Fig. 2 and is typical of all the symmetric flow patterns. In Fig. 10b, the left primary center of coalescence and the saddle point below it start lifting away from the surface. At the same time, the right-hand structure moves toward the leeward meridian. The images at $Re_D = 1.2\times10^5$ and $x/D = 1.0$ or 2.0 in Fig. 4 are two examples of this geometry. As the flow structure becomes more asymmetric, the right-hand center moves further to the left under the detaching structure, as shown in Fig. 10c. As a result, two nodes around which the fluid rotates in the same, counterclockwise, direction move closer to each other. The images at $Re_D = 2\times10^5$ and $x/D = 1.0$ in Fig. 4, as well as Fig. 9, are two samples of this stage. This topology sketch explains the occurrence of what has been defined before as the expansion of the reattachment line to a wide region (the shaded lines in Fig. 8). This expansion is actually the space between the saddle points that enclose the counterclockwise secondary structure and its appearance is a direct result of the developing asymmetry.

The break in the stream surfaces, the formation of two distinct detached foci, and the appearance of a third center are demonstrated in Fig. 10d. This sketch corresponds to the flow structure at $x/D = 1.0$ and $Re_D = 2.4\times10^5$ as well as 2.8×10^5 (third and fourth row of Fig. 4). Variations in the relative lo-

cation of the nodes are demonstrated in Fig. 10e, which corresponds to the image at $x/D=2.0$ when the Re_D is 2.8×10^5. This sketch also outlines the complete detachment of these centers as the line connecting the upper saddle point and the surface is "torn" and "drawn" into the upper node. Finally, the recombination of the split structures, the initial stages of detachment of the right primary center of converging stream surfaces, and the motion of the new left hand focus toward the leeward meridian are presented in Fig. 10f. This sketch corresponds to the flow structures at $x/D=3.0$ for Reynolds numbers between 2.0×10^5 and 2.8×10^5. This sketch also contains speculated, newly formed, secondary structures on the left-hand side of the model.

As we have already noted, the qualitative sketches in Fig. 10 represent typical patterns that have been observed during the current experiments. The actual location of the nodes and the saddle points depend on the Reynolds number and the incidence angles. The variations in the location, as well as the number of the primary nodes (primary centers of coalescence), are presented in Figs. 5 and 6, whereas the surface saddle points are specified in Fig. 8. Due to the length of this paper, we cannot include more information here. Future publications, currently in preparation, will follow the evolution of all the nodes as well as the saddle points with the Reynolds number and the axial location.

Summary and Conclusions

Laser-induced fluorescence has been utilized for visualizing the intricate details of the flow structures behind an inclined body of revolution. The observations have focused on the effects of the incidence angle and the Reynolds number on the axial development of the foci or the "centers of coalescing stream surfaces" as well as the location of boundary-layer separation and reattachment. At low angles of incidence and low Reynolds numbers, the flow is symmetric, containing two large centers (foci) of coalescence as well as several secondary structures. The transition to an asymmetric flow has been observed to begin first in the downstream sections with the gradual lifting of the left primary center and an inward motion of the right-hand structure. This motion also involves a delay in the location of boundary-layer separation on the right-hand side and a motion of the line separating between the primary structures toward the left side of the model. While detaching, the left structure becomes elongated as the stream surfaces break and start coalescing into distinct centers. The resulting two foci then start interlacing around each other and eventually recombine further downstream. At the same time, the right-hand focus moves under the detaching structure toward a secondary center that rotates in the same direction. The resulting image gives the impression that the line separating the primary structures expands into a wide region. As the left center detaches, the small secondary structure below it grows and occupies the vacated space. The detachment of coalescing stream surfaces on the right-hand side follows in a similar manner. Evidence of asymmetry very close to the tip of the model at 45 deg incidence is also provided. Finally, this paper includes qualitative drawings of the flow topology, which follow the evolution of the flow structures in the lee of the model.

Acknowledgment

This work has been supported by the National Science Foundation under Contract MEA-840443. Their support is gratefully acknowledged. The authors would also like to thank Tom Cooper and Tom Frances for their help in the construction of the facility.

References

[1]Allen, H. J. and Perkins, E. W., "A Study of Effects of Viscosity on Flow Over Slender Inclined Bodies of Revolution," NACA Rept. 1048, 1951.

[2]Allen, H. J. and Perkins, E. W., "Characteristics of Flow Over Inclined Bodies of Revolution," NACA RM-A50L07, March 1951.

[3]Pick, G. S., "Investigation of Side Force on Ogive-Cylinder Bodies at High Angles of Attack in the $M=0.5$ to 1.1 Range," AIAA Paper 71-0570, June 1971.

[4]Thomson, K. D. and Morrison, D. F., "The Spacing, Position and Strength of Vortices in the Wake of Slender Cylindrical Bodies at Large Incidence," *Journal of Fluid Mechanics*, Vol. 50, No. 4, 1971, pp. 751-783.

[5]Coe, P. L., Jr., Chambers, J. R., and Letko, W., "Asymmetric Lateral-Directional Characteristics of Pointed Bodies of Revolution at High Angles of Attack," NASA TN-D-7095, Nov. 1972.

[6]Keener, E. R. and Chapman, G. T., "Onset of Aerodynamic Side Forces at Zero Sideslip on Symmetric Forebodies at High Angles of Attack," AIAA Paper 74-0770, Aug. 1974.

[7]Lamont, P. J. and Hunt, B. L., "Pressure and Force Distributions on a Sharp-Nosed Circular Cylinder at Large Angles of Inclination to a Uniform Subsonic Stream," *Journal of Fluid Mechanics*, Vol. 76, Aug. 1976, pp. 519-559.

[8]Jorgensen, L. H., "Prediction of Aerodynamic Characteristics for Slender Bodies Alone and with Lifting Surfaces to High Angles of Attack," AGARD CP-247, Oct. 1978, Paper 28.

[9]Dexter, P. C. and Hunt, B. L., "The Effects of Roll Angle on Flow Over a Slender Body of Revolution at High Angles of Attack," AIAA Paper 81-0358, Jan. 1981.

[10]Dexter, P. C., "A Study of Asymmetric Flow Over Slender Bodies at High Angles of Attack in a Low Turbulence Environment," AIAA Paper 84-0505, Jan. 1984.

[11]Ericsson, L. E. and Reding, J. P., "Asymmetric Vortex Shedding from Bodies of Revolution," *Tactical Missile Aerodynamics, AIAA Progress in Astronautics and Aeronautics*, Vol. 104, edited by M. J. Hemsch and J. N. Nelson, AIAA, New York, 1986, pp. 243-296.

[12]Yanta, W. J. and Wardlaw, A. B., "Laser Doppler Velocimeter Measurements of Leeward Flowfields on Slender Bodies at Large Angle-of-Attack," AIAA Paper 77-0660, Jan. 1977.

[13]Oberkampf, W. L. and Bartel, T. J., "Symmetric Body Vortex Wake Characteristics in Supersonic Flow," AIAA Paper 78-1337, 1978.

[14]Owen, F. K. and Johnson, D. A., "Wake Vortex Measurements of Bodies at High Angle of Attack," AIAA Paper 78-0023, Jan. 1978.

[15]Keener, E. R., "Oil-Flow Separation Patterns on an Ogive Forebody," NASA TM-81314, Oct. 1981.

[16]Newsome, R. W. and Kandil, O. A., "Vortical Flow Aerodynamics-Physical Aspects and Numerical Simulation," AIAA Paper 87-0205, Jan. 1987.

[17]Hall, R. M., "Forebody and Missile Side Forces and the Time Analogy," AIAA Paper 87-0327, 1987.

[18]Schwind, R. G. and Mullen, J., "Laser Velocimeter Measurements of Slender-Body Wake Vortices," AIAA Paper 79-0302, Jan. 1979.

[19]Oberkampf, W. L., Owen, F. K., and Shivananda, T. P., "Experimental Investigation of the Asymmetric Body Vortex Wake," AIAA Paper 80-0174, Jan. 1980.

[20]Wardlaw, A. B. and Yanta, J. W., "The Flow Field About and Forces on Slender Bodies at High Angles of Attack," AIAA Paper 80-0184, Jan. 1980.

[21]Yanta, W. J. and Wardlaw, A. B., "Multi-Stable Vortex Patterns on Slender, Circular Bodies at High Incidence," AIAA Paper 81-0006, Jan. 1981.

[22]Wardlaw, A. B. and Yanta, W. J., "Asymmetric Flowfield Development on a Slender Body at High Incidence," *AIAA Journal*, Vol. 2, Feb. 1984, pp. 242-249; also AIAA Paper 82-0343, Jan. 1982.

[23]Nielsen, J. N., "Nonlinearities in Missile Aerodynamics," AIAA Paper 78-0020, Jan. 1978.

[24]Wardlaw, A. B., Jr., "High Angle of Attack Missile Aerodynamics," AGARD LS-98, March 1978, Paper 5.

[25]Peake, D. J. and Tobak, M., "Three-Dimensional Interactions and Vortical Flows with Emphasis on High Speeds," AGARD AG-252, July 1980.

[26]Hunt, B. J., "Asymmetric Vortex Forces and Wakes on Slender Bodies," AIAA Paper 82-1336, Aug. 1982.

[27]Settles, G. S., "Modern Developments in Flow Visualization," AIAA Paper 84-1599, June 1984.

[28]Werle, H., "Flow Visualization Techniques for the Study of High Incidence Aerodynamics," AGARD LS-121, No. 3, Dec. 1982.

[29]Dewey, C. F., Jr., "Qualitative and Quantitative Flow Field Visualization Utilizing Laser Induced Fluorescence," AGARD CP-193, No. 17, 1976.

[30]Gad-el-Hak, M., "The Use of Dye Laser Technique for Unsteady Flow Visualization," *Journal of Fluids Engineering*, Vol. 108, 1986, pp. 34–48.

[31]Katz, J., Frances, T. B., and Ward, K. C., "Flow Visualization Studies in a Towing Tank Using Laser Induced Fluorescence," *ASME Fluid Measurements and Instrumentation Forum*, Vol. 34, May 1986, pp. 57–59.

[32]Ward, K. C., "A Flow Visualization Study Around a 3.5 *l/D* Ogive at High Angles of Incidence," M.S. Thesis, Purdue Univ., West Lafayette, IN, Aug. 1987.

[33]Moore, D. W. and Saffman, P. G., "Structure of a Line Vortex in Imposed Strain," *Aircraft Wake Turbulence*, edited by J. H. Olsen, A. Goldburg, and M. Rogers, Plenum, New York, 1971, pp. 339–354.

[34]Freymuth, P., Bank, W., and Palmer, M., "Further Experimental Evidence of Vortex Splitting," *Journal of Fluid Mechanics*, Vol. 152, 1985, pp. 289–299.

[35]Tobak, M. and Peake, D. J., "Topology of Two-Dimensional and Three-Dimensional Separated Flows," AIAA Paper 79-1480, July 1979.